nature communications

Article

https://doi.org/10.1038/s41467-026-69730-4

# Modulating TPP riboswitch activity simultaneously enhances crop yield, nutritional quality and stress tolerance

Received: 17 March 2025

Accepted: 9 February 2026

Published online: 28 February 2026

Check for updates

Yufei Li[1,2,7], Kang Li[2,3,7], Jiazhi Lu[1,7], Mustafa Bulut[4,5,7], Huanteng Hou[1,2], Qamar U. Zaman[1], Ran Zhang[1,2], Zhuang Yang[2], Chenkun Yang[1], Chuansong Zhan[1], Guan Wang[1], Tong Chen[1,2], Xianqing Liu[2], Qiao Zhao[6], Shuangqian Shen[1] ✉, Alisdair R. Fernie[4] ✉ & Jie Luo[1,2] ✉

While enhancing crop yield remains a critical breeding objective, such efforts often compromise nutritional quality and stress tolerance. The growing global population and increasing environmental stresses make combining stable crop yields with improved nutritional quality a vital objective for sustainable food security. Thiamine pyrophosphate (TPP), the active form of vitamin B1, regulates core metabolism to support both human health and plant stress tolerances. Here, we show that editing the rice TPP riboswitch elevates multiple micronutrients, simultaneously increasing grain yield, cold tolerance, and blast resistance. Mechanistically, these enhancements link to promoted photosynthesis, improved nitrogen use efficiency, and system-wide transcriptional-metabolic reprogramming. Editing homologs in tomato produces similar outcomes, supporting the generalizability of this approach. Thus, modulating TPP levels offers a viable strategy to synergistically boost crop productivity, nutritional quality, and stress tolerance, which are essential for achieving sustainable food security without trade-offs.

Food security, defined as the sustainable access to sufficient and nutritious food, is a fundamental pillar of global health and socioeconomic stability[1,2]. The urgency to ensure food security is escalating, driven by a surging global population, diminishing arable land, and increasing climate extremes, which collectively pose substantial threats to agricultural productivity[3–5]. Current strategies to address food security prioritize dual objectives: enhancing crop yields under both optimal and adverse conditions and improving nutritional quality[6–8]. However, simultaneously achieving these objectives remains a major challenge, as most research efforts have focused on improving single traits, often overlooking the inherent trade-offs between yield, nutritional content, and stress resistance.

Over the past three decades, metabolic engineering and gene editing techniques have been utilized to create a variety of biofortified crops to address nutritional deficiencies in the global population. Notable examples include "Golden Rice" enriched with β-carotene[9], riboflavin-rich rice[10], pyridoxine-enriched rice[11], folate-fortified rice[12], 7-dehydrocholesterol-rich tomato[13], lysine-enhanced maize[14], anthocyanin-rich rice[15], and astaxanthin-containing rice[16]. Although these efforts hold potential for addressing specific micronutrient deficiencies in particular regions or countries, their practical

[1]Yazhouwan National Laboratory, Sanya, China. [2]School of Breeding and Multiplication (Sanya Institute of Breeding and Multiplication), Hainan University, Sanya, China. [3]School of Tropical Agriculture and Forestry, Hainan University, Danzhou, China. [4]Max Planck Institute of Molecular Plant Physiology, Potsdam-Golm, Germany. [5]Program Center MetaCom, Leibniz Institute of Plant Biochemistry, Halle (Saale), Germany. [6]Shenzhen Key Laboratory of Synthetic Genomics, Guangdong Provincial Key Laboratory of Synthetic Genomics, Key Laboratory of Quantitative Synthetic Biology, Shenzhen Institute of Synthetic Biology, Shenzhen Institute of Advanced Technology, Chinese Academy of Sciences, Shenzhen, China. [7]These authors contributed equally: Yufei Li, Kang Li, Jiazhi Lu, Mustafa Bulut. ✉e-mail: shenshuangqian@yzwlab.cn; fernie@mpimp-golm.mpg.de; jie.luo@hainanu.edu.cn

implementation faces substantial nonscientific constraints, including regulatory barriers, public scepticism, and market access limitations. For instance, Golden Rice, developed over two decades ago, has been repeatedly delayed and even withdrawn from certain markets due to public attitudes and political factors, rather than widely alleviating vitamin A deficiency as initially envisioned[17]. Moreover, the capacity and transformation efficiency of gene expression vectors are generally insufficient[18], making it difficult to achieve synergistic enrichment of multiple nutrients in crops, thus failing to solve the main problem of "hidden hunger" affecting nearly 2 billion people–worldwide, reflecting deficiencies in multiple essential nutrients within staple crops. Therefore, the broader and more persistent challenge remains to explore important genetic breeding strategies that have greater public acceptance and can be used to address the crisis of micronutrient deficiencies in populations.

Beyond these implementation barriers, intrinsic biological constraints, specifically genetic and physiological trade-offs, further complicate the simultaneous improvement of multiple desirable traits. Pleiotropic effects often lead to unintended consequences[19–21]. For example, the Green Revolution gene *sd1* (*semi-dwarf 1*) increased the harvest index in rice but reduced nitrogen use efficiency and drought tolerance[22]. Similarly, mutagenesis of the GL4 gene in rice increased shattering resistance but resulted in a relatively small grain size[23]. In wheat, the dwarfing allele *Rht-B1b* improved lodging resistance at the cost of root biomass and water uptake capacity[24]. Plant immune responses also illustrate this dilemma: pathogen recognition receptors such as *Xa21* in rice confer blast resistance but can reduce grain size under pathogen-free conditions, and salicylic acid-mediated defence signalling often represses growth through crosstalk with gibberellin pathways[25,26]. Although conventional breeding and transgenic strategies can partially mitigate linkage drag, gene pleiotropy-driven trade-offs remain a fundamental obstacle to crop improvement. Accordingly, identifying genetic loci that break the trade-offs between yield, stress resistance, and nutritional quality is of vital importance for addressing food security.

Thiamine (vitamin B1) plays a pivotal role in central energy metabolism in both animals and plants. In humans, its deficiency is associated with severe neurological and cardiovascular disorders[27–29]. In plants, thiamine sustains the continuous supply of ATP and acetyl-CoA essential for almost all life activities by maintaining the activity of several core enzymes in the pentose phosphate pathway, the Calvin–Benson cycle, and the tricarboxylic acid (TCA) cycle through its active form, thiamine pyrophosphate (TPP). In addition to its metabolic functions, vitamin B1 also acts as a priming agent for defence responses, inducing systemic acquired resistance (SAR) and pathogenesis-related (PR) gene expression through the salicylic acid and $Ca^{2+}$ signalling pathways in diverse species, including rice, tobacco, tomato, and *Arabidopsis*[30–34]. Furthermore, vitamin B1 contributes to photosynthetic efficiency, chloroplast homeostasis, and mitigation of abiotic stress by reducing reactive oxygen species accumulation[28,35,36]. Vitamin B1 biosynthesis in plants is regulated via TPP riboswitches, conserved structured RNA elements located in the 3′-UTR of *THIC* that sense cellular TPP levels to feedback-inhibit biosynthesis[37,38]. Mutations in these riboswitch elements have been shown to increase thiamine and TPP levels by 5–10 times[39], thereby influencing carbon/nitrogen metabolism and stress responsiveness[40]. All the positive effects of vitamin B1 and the regulatory role of riboswitches on vitamin B1 suggest that mediating TPP riboswitches may regulate crop growth, resistance, and metabolic flux by altering the homeostasis of vitamin B1. However, the application potential of this regulatory mechanism for the coordinated improvement of multiple traits in crops remains unexplored in prior research.

In this study, we address this knowledge gap by employing CRISPR-Cas9-mediated editing of the TPP riboswitch in rice to reprogram vitamin B1 homeostasis. We demonstrate that this intervention leads to synergistic enhancements in grain nutritional quality, yield, cold tolerance, and blast resistance. Mechanistic studies reveal that these improvements are underpinned by augmented photosynthetic capacity, optimized nitrogen utilization, and systemic transcriptional–metabolic reprogramming. The recapitulation of key phenotypes in tomato further underscores the broad applicability of this strategy. Importantly, our approach overcomes the pervasive trade-offs inherent in conventional breeding and enables the coordinated improvement of productivity, nutritional quality, and environmental resilience via a single genetic modification. This transgene-free TPP riboswitch-mediated gene editing strategy provides a promising approach for crop improvement that contribute to sustainable food security and is easy to be accepted by the public.

## Results

### Targeted editing of TPP riboswitch elevates thiamine and broad-spectrum micronutrients in rice

To enhance vitamin B1 level in rice, we employed a CRISPR-Cas9 system to edit the TPP riboswitch in the 3′-UTR of *OsTHIC*, the key enzyme for vitamin B1 synthesis. Seven vectors, each harbouring one or two designed single guide RNAs targeting the TPP riboswitch and its flanking sequences on *OsTHIC*, were transformed into Zhonghua 11 (ZH11). Totally, 47 out of 173 $T_0$ lines carried mutations. After two generations of self-pollination, we isolated nine homozygous $T_2$ lines, named *trs1* to *trs9*. These mutants encompassed various mutation types, including deletions ranging from 1 to 231 bp and a 241-bp insertion in the TPP riboswitch (Fig. 1a, Supplementary Fig. 1 and Supplementary Data 1). All the nine lines showed significant increases in the vitamin B1 content in different tissues, with *trs3* and *trs8* displaying the highest thiamine contents (Fig. 1b-d). Quantitatively analysis of polished rice revealed that the thiamine content increased from 0.92 mg $kg^{-1}$ in ZH11 to 5.26 mg $kg^{-1}$ and 5.51 mg $kg^{-1}$ in *trs3* and *trs8*, respectively (Fig. 1e).

Given that vitamin B1 supplies upstream precursors for multiple nutrients by governing glycolysis and the tricarboxylic acid (TCA) cycle, we performed targeted metabolomic profiling of 115 nutrients and health-related components in polished rice, including 17 vitamins, 53 lipids, 21 amino acids, nine sugars and 15 polyphenols. As expected, most nutrients in the *trs3* and *trs8* were significantly higher than those in ZH11 (Fig. 1f, Supplementary Data 2). These included riboflavin, niacin, pantothenic acid, pyridoxine, α-tocopherol, monoacylglycerophospholipids, and several amino acids that human dietary-essential (Fig. 1g-q). We also analysed the macronutrient contents and detected no significant differences in total starch or grain protein levels between the *trs* lines and ZH11 (Supplementary Fig. 2), indicating that the nutritional enhancement was specific to micronutrients and did not affect the core energy or protein value of the rice. These results suggest that gene editing of the TPP riboswitches can simultaneously increases the levels of both vitamin B1 and a broad spectrum of other nutrients without altering the fundamental macronutrient composition in rice.

### TPP riboswitch editing boosts grain yield via improved panicle architecture in rice

To evaluate the agronomic traits of riboswitch-edited plants, we conducted field trials in Wuhan using *trs3*, *trs8*, and ZH11 plants (Fig. 2a-c). Compared with ZH11, the *trs3* and *trs8* exhibited significant increases in plot yield, ranging from 19.29–20.77% (Fig. 2d), and the height of the edited lines during the reproductive period also significantly increased (Fig. 2e, Supplementary Fig. 3). In contrast, the mutants and ZH11 showed comparable performance in thousand-grain weight, grain shape (including grain length, width, or thickness), tiller number, and panicle number per plant (Fig. 2f, g, Supplementary Fig. 4a-d). To further exclude the possibility that the increased yield was caused by

https://doi.org/10.1038/s41467-026-69730-4

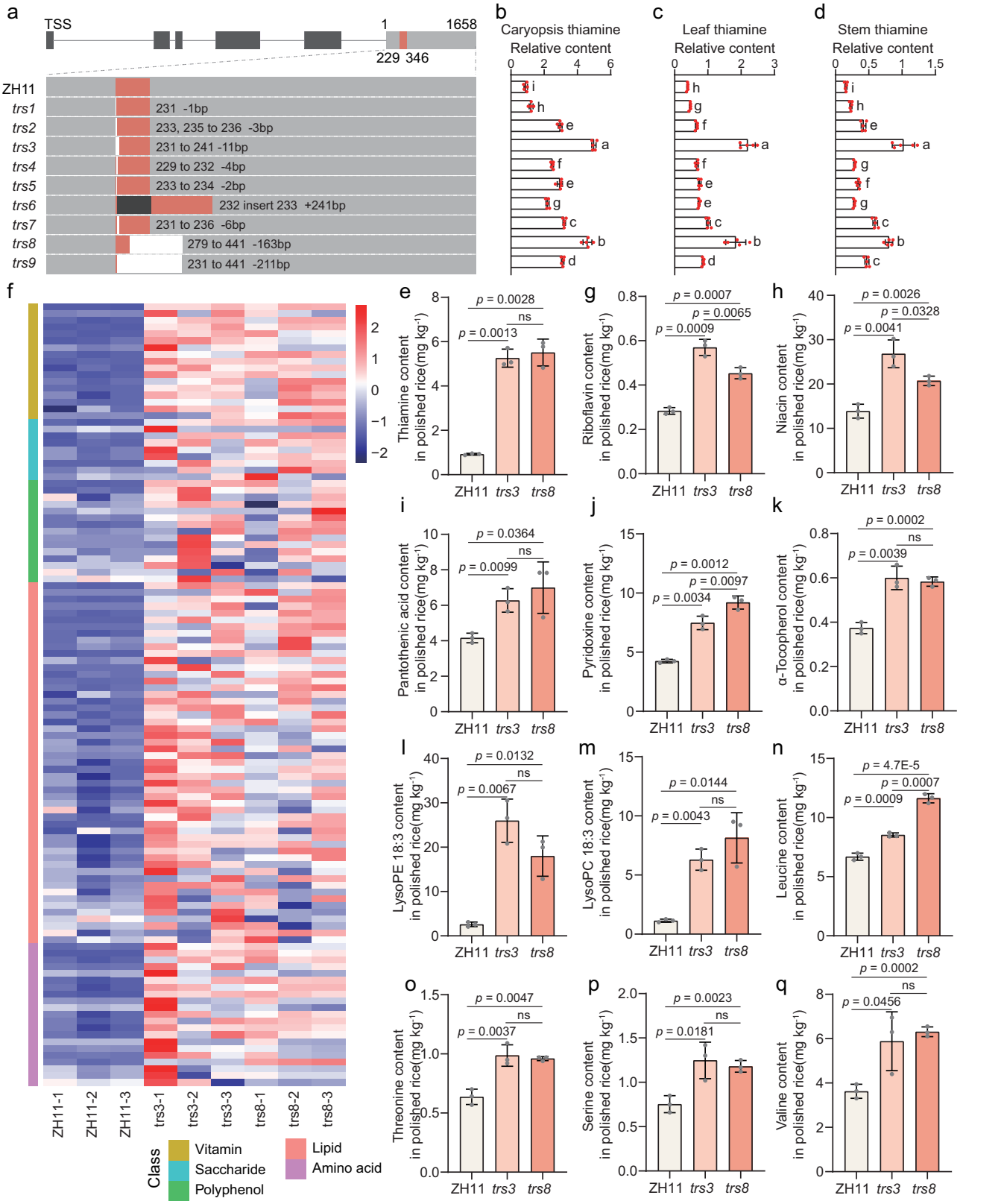


**Fig. 1 | Increased contents of multiple nutrients in the TPP riboswitch gene edited lines. a–d** Nine gene-edited types of TPP riboswitches (**a**) and the relative thiamine content (intensity by LC-MS/MS, c.p.s, ×10$^6$) of each type in caryopsis (**b**), leaf (**c**), and stem (**d**). **e** Quantification of thiamine in polished rice of ZH11, *trs3* and *trs8* lines. **f** Comparative analysis of metabolite profiles in polished rice of ZH11 and *trs* lines. Data for each row is standardized by *Z*-score. **g–q** Quantification of riboflavin, niacin, pantothenic acid, pyridoxine, α-tocopherol, lysoPE 18:3, lysoPC 18:3, leucine, threonine, serine, valine in polished rice of ZH11, *trs3* and *trs8* lines. Bars represent mean ± SD, with error bars show variability among biological replicates, and gray dots indicate individual samples. Data in (**b–d**) (ZH11, $n = 5$; *trs* - *trs9*, $n = 5$ per line), in (**e**, **g–q**) (ZH11, $n = 3$; *trs3*, $n = 3$; *trs8*, $n = 3$). All statistical tests were carried out using a one-way ANOVA, with distinct letters indicating significant differences ($P < 0.05$). Source data are provided as a Source Data file.

https://doi.org/10.1038/s41467-026-69730-4

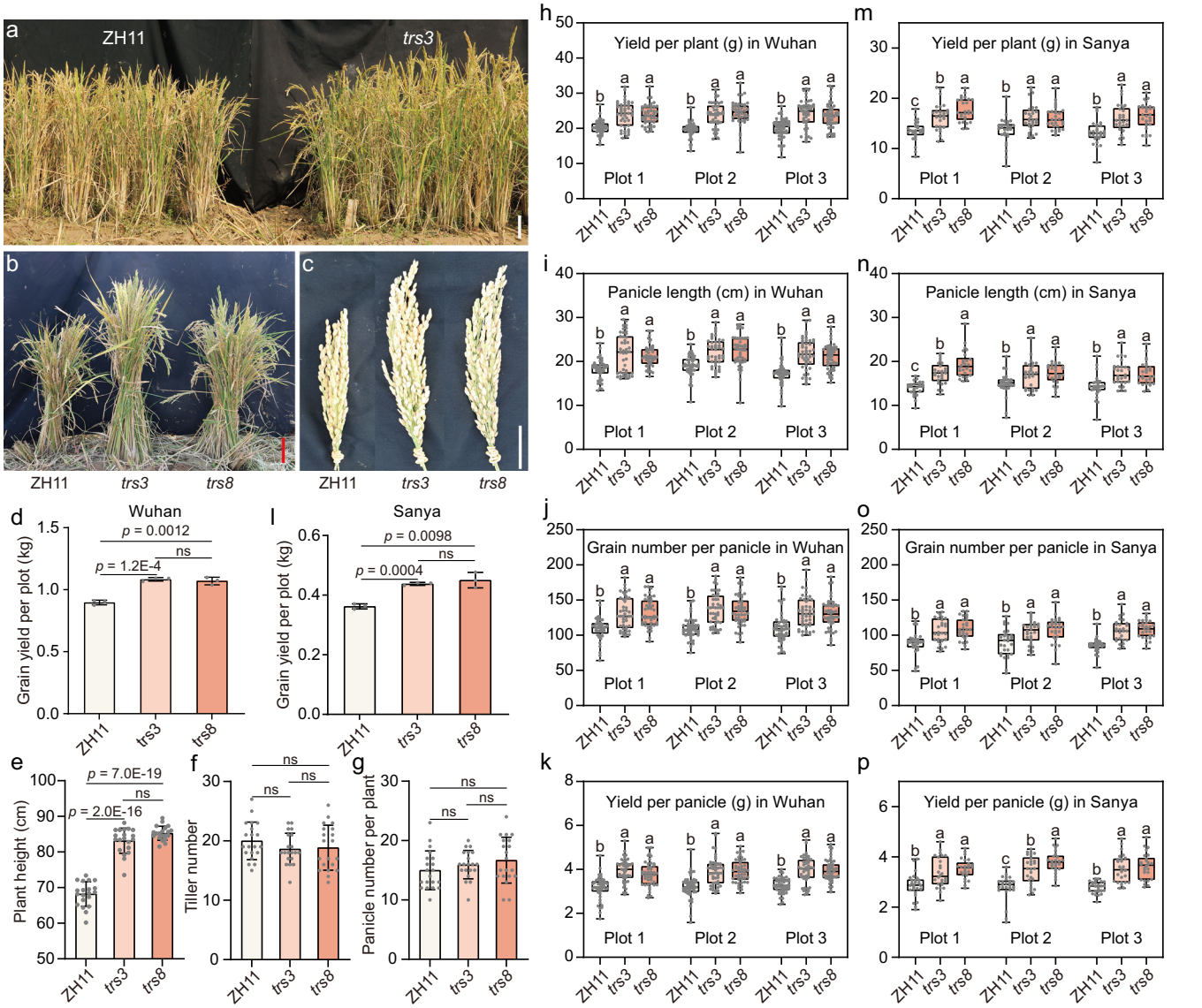


**Fig. 2 | *trs* rice lines showed increased yield related parameters. a–c** Phenotypes of ZH11, *trs3* and *trs8* plants grown in Wuhan in 2023. Scales bar represent 10 cm (**a**, **b**) and 5 cm (**c**). **d–p** Yield-related traits of ZH11and *trs* mutant lines cultivated in Wuhan in 2023 (**d–k**) and Sanya in 2024 (**l–p**). Measured parameters include: grain yield per plot (**d, l**), yield per plant (**h, m**), panicle length (**i, n**), grain number per panicle (**j, o**), yield per panicle (**k, p**). **e, f** Statistical analysis of plant height (**e**), tiller number (**f**) and panicle number per plant (**g**) of ZH11, *trs3* and *trs8* lines cultivated in Wuhan (2023). Panicle-related data were recorded for the main panicle of individual plants. In the bar chart, bars represent the mean ± SD, whereas in the box plot, whiskers represent the data range and the center line represents the median. In both plots, error bars denote variability among biological replicates, and gray dots indicate individual samples. Data in (**d**) ($n = 3$ plots, 50 plants within a plot), in (**e–g**) (ZH11, $n = 20$; *trs3*, $n = 20$; *trs8*, $n = 20$), in (**h**) (plot1, $n = 47$ per line; plot2, $n = 45$ per line; plot3, $n = 50$ per line), in (**i**) (plot1, $n = 44$ per line; plot2, $n = 45$ per line; plot3, $n = 49$ per line), in (**j**) (plot1, $n = 45$ per line; plot2, $n = 47$ per line; plot3, $n = 48$ per line), in (**k**) (plot1, $n = 45$ per line; plot2, $n = 48$ per line; plot3, $n = 47$ per line), in (**l**) ($n = 3$ plots, 30 plants within a plot), in (**m**) (plot1, $n = 27$ per line; plot2, $n = 29$ per line; plot3, $n = 29$ per line), in (**n**) (plot1, $n = 26$ per line; plot2, $n = 29$ per line; plot3, $n = 28$ per line), in (**o**) (plot1, $n = 28$ per line; plot2, $n = 28$ per line; plot3, $n = 27$ per line), in (**p**) (plot1, $n = 26$ per line; plot2, $n = 26$ per line; plot3, $n = 26$ per line). All statistical tests were carried out using a one-way ANOVA, with distinct letters indicating significant differences ($P < 0.05$). Source data are provided as a Source Data file.

planting density, we conducted phenotypic analyses of individual plant traits in three separated and randomized plots. The results indicated that compared with ZH11, *trs3* and *trs8* led to 17.80–25.27% increases in grain yield per plant (Fig. 2h). A detailed phenotypic analysis revealed that the increases in yield in the *trs3* and *trs8* lines correlated with 16.33–26.42% increases in panicle length compared with that in ZH11 (Fig. 2c, i), which correspondingly increased the number of grains and yield per panicle (Fig. 2j, k).

To assess the stability of the yield enhancement conferred by the TPP riboswitch edits, we conducted field trials in Sanya, which represents a very different environmental setting. Despite the contrasting conditions, compared with ZH11, *trs3* and *trs8* lines still showed significant yield improvements under short-day and tropical conditions in Hainan, with yield increases ranging from 20.79–24.29% per plot and 17.31–31.19% per plant, respectively (Fig. 2l, m). Additionally, the panicle length, grain number and yield per panicle of *trs3* and *trs8* lines were significantly higher compared to ZH11 (Fig. 2n-p, Supplementary Fig. 5). Taken together, these results indicate that editing the TPP riboswitch enhances grain yield, which is associated with improved panicle architecture.

https://doi.org/10.1038/s41467-026-69730-4

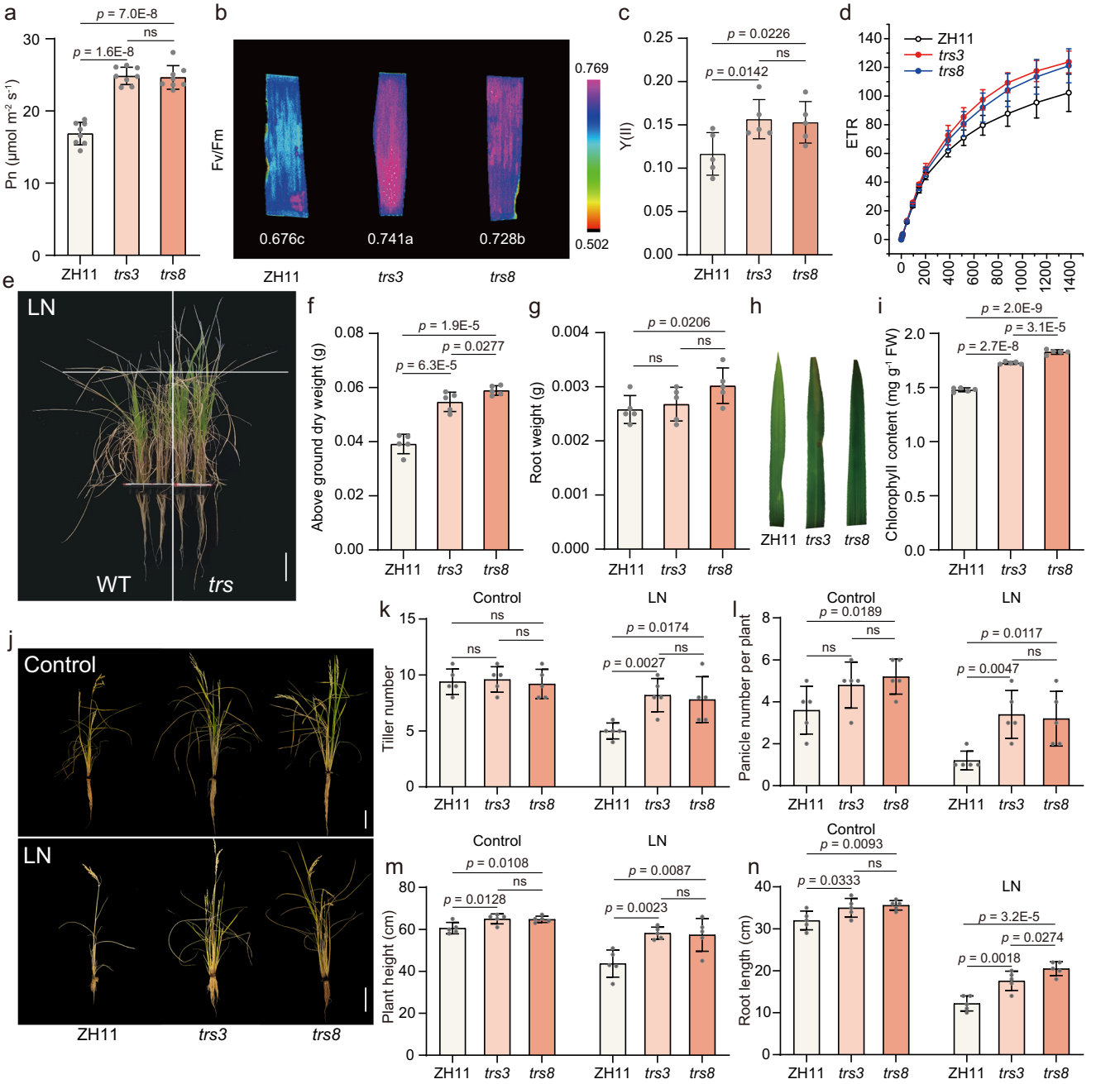


**Fig. 3 | The gene-edited TPP riboswitch improves photosynthetic capacity and nitrogen utilization. a** Net photosynthetic rate (Pn). **b** Maximum photochemical efficiency of PSII (Fv/Fm). **c** Effective quantum yield of PSII photochemistry [Y(II)]. **d** The electron transfer rate of photosystem (ETR). The abscissa represents different light intensities (μmol $m^{-2}$ $s^{-1}$). **e** Phenotypes of WT (first two rows), *trs3* (third row) and *trs8* (fourth row) mutant plants under limited N conditions. Scale bar = 5 cm. **f** Above ground dry weight of WT and trs plants under limited N conditions. **g** Root dry weight of WT and *trs* mutant plants under limited N conditions. **h** Leaves Phenotypes of WT and *trs* mutant plants under limited N conditions. **i** The chlorophyll content in the leaves of WT and *trs* plants. **j** Phenotypes of ZH11 and *trs* mutants under limited N conditions throughout the plant growth period. Left to right: ZH11, *trs3*, and *trs8*. Scale bar = 10 cm. **k** Tiller number of WT and *trs* mutant plants under limited N conditions. **l** Panicle number per plant of WT and *trs* mutants under limited N conditions. **m** Plant height of WT and *trs* mutants under limited N conditions. **n** Root length of WT and *trs* plants under limited N conditions. Bars represent mean ± SD, with error bars show variability among biological replicates, and gray dots indicate individual samples. Data in (**b**) ($n = 8$ per line), in (**c**, **f**, **g**, **i**, **k**, **l**-**n**) ($n = 5$ per line). All statistical tests were carried out using a one-way ANOVA. ns, Not significant ($P > 0.05$). Source data are provided as a Source Data file.

## Enhanced photosynthetic capacity and nitrogen use efficiency underlie yield improvement

To disclose the physiological mechanism underling the elevated yield in gene edited lines, we characterized key aspects of photosynthesis. Compared with ZH11, the *trs3* and *trs8* lines exhibited a 46.01–47.27% higher photosynthesis rates under standard growth conditions (Fig. 3a). Additionally, these plants presented elevated Fv/Fm values (which represent the maximum quantum efficiency of photosystem II when all the capable reaction centres are open) and increased photosystem II yields (Fig. 3b, c). Furthermore, the gene-edited riboswitch lines displayed elevated rates of chloroplast electron transport (Fig. 3d, Supplementary Fig. 6).

https://doi.org/10.1038/s41467-026-69730-4

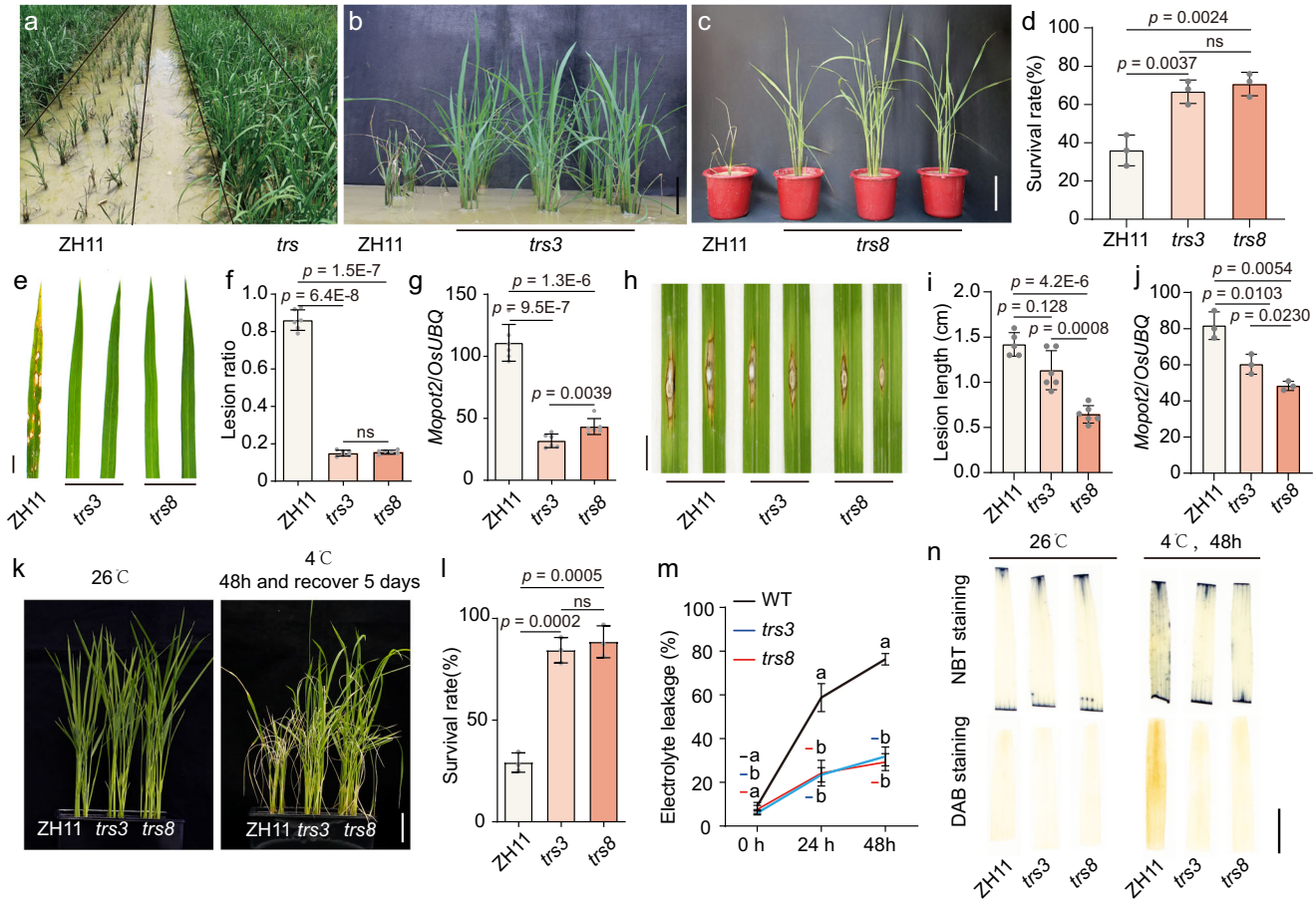


**Fig. 4 | The gene-edited TPP riboswitch increased rice blast disease and cold resistance. a** Field phenotypes of ZH11 and *trs* lines at tillering under natural disease pressure in Taojiang. The gray line demarcates the *trs3* lines (above) from the *trs8* lines (below). **b**, **c** Detailed phenotypic comparison of ZH11, *trs3* lines (**b**), and the *trs8* lines (**c**) under natural disease pressure in Taojiang. Scale bar in (**b, c**), 10 cm. **d** The survival rates of ZH11, *trs3* lines, and the *trs8* lines under natural disease pressure in Taojiang. **e**–**g** Analysis of disease lesion area ratio (**f**) and fungal biomass (**g**) in rice plants at 10 days after spray inoculation with *Magnaporthe oryzae* (strain ZB25). $n = 6$ per line. With respect to fungal growth, Mopot2 expression was measured by qRT–PCR, and the expression in the inoculated leaves was normalized to that of *OsUbQ*. **h**–**j** Assessment of lesion length (**i**) and fungal biomass (**j**) in rice plants at 10 days after needle punch inoculation with blast fungus strain ZB25. Data in (**h**, **i**) (ZH11, $n = 5$; *trs3*, $n = 6$; *trs8*, $n = 6$), in (**j**) ($n = 3$ per line). **k** Phenotypes of ZH11 and *trs* mutant lines under control (26 °C) and after cold stress (48 h at 4 °C) followed by a 5-day recovery period. Scale bar, 5 cm. **l** The survival rate of ZH11 and *trs* lines after cold stress. $n = 3$ per line. **m** The electrolyte leakage in ZH11 and *trs* lines under cold stress. $n = 3$ per line. **n** ROS accumulation detected by DAB and NBT staining in ZH11, *trs3*, and *trs8* leaves under cold stress. ROS, reactive oxygen species. Bars represent mean ± SD, with error bars show variability among biological replicates, and gray dots indicate individual samples. Statistical significance was determined by one-way ANOVA, with distinct letters indicating significant differences ($P < 0.05$). Source data are provided as a Source Data file.

We further evaluated plant performance under limited nitrogen (LN) conditions under hydroponics, providing only 20% of the nitrogen provided under control conditions. Under LN stress, the *trs3* and *trs8* lines presented significantly greater aboveground biomass under LN conditions and a slightly greater root biomass than the wild type (Fig. 3e-g). Concurrently, chlorophyll content in the edited lines was 16.73–23.62% higher than in ZH11 (Fig. 3h, i). When the LN treatment was maintained throughout the reproductive stage (from flowering to maturity), striking phenotypic differences emerged between the mutants and wild type (Fig. 3j). Compared with WT, the *trs* lines produced more tillers, panicles per plant, plant height, and root length under LN conditions (Fig. 3k-n).

## Riboswitch editing confers dual resistance to blast and cold stress

To evaluate the stress tolerance of the riboswitch-edited lines, we first performed field trials under natural blast (*Magnaporthe oryzae*) pressure in Taojiang, Hunan Province, a blast-endemic region. Under standard cultivation, the *trs3* and *trs8* lines demonstrated enhanced resistance to natural pathogen infection compared with the wild-type ZH11 (Fig. 4a-d). The stability of this resistance was confirmed in a second-year trial in Enshi, Hubei Province, where the mutants exhibited significantly lower disease incidence and severity than ZH11 (Supplementary Fig. 7).

We also conducted controlled infection assays using two distinct inoculation methods: spray inoculation (simulating natural spore dispersal) and punch inoculation (localized tissue penetration) with *M. oryzae* (ZB25 strain). Spray inoculation revealed that the edited lines developed significantly shorter lesion lengths than ZH11, which displayed typical blast lesions (Fig. 4e, f). The same resistant-phenotype was also consistently observed in the punch inoculation (Fig. 4h, i). Quantitative PCR analysis of fungal biomass confirmed these morphological observations, showing a significant reduction in *M. oryzae* DNA in riboswitch-edited lines relative to ZH11 under both inoculation methods (Fig. 4g, j). Furthermore, we conducted additional inoculation trials using distinct pathogen strains isolated from the northern (Liaoning) and southern (Enshi) regions of China. In these assays, the riboswitch-edited lines

consistently exhibited a clear disease-resistant phenotype (Supplementary Fig. 8).

Low temperature (LT) threatens rice growth and productivity, largely through induced oxidative stress that harms plants[41–43]. Vitamin B1 biosynthetic genes are known to play important roles in plant resistance to various oxidative stresses. Transcriptomic data from maize have shown that the expression levels of most vitamin B1 synthesis pathway genes are induced by LT[44]. Similarly, we observed marked upregulation of multiple vitamin B1 biosynthetic genes, including *OsTHIC*, in rice under cold stress (Supplementary Fig. 9). This prompted us to test the cold tolerance of the *trs* mutants. When subjected to LT treatment, the *trs3* and *trs8* lines displayed visibly less leaf rolling than ZH11 (Supplementary Fig. 10). Following a 2-day cold treatment and recovery, more than 84% of the riboswitch-edited lines survived, compared with only approximately 29% of ZH11 plants (Fig. 4k right, 4 l). The *trs* mutants showed significantly slower electrolyte leakage than ZH11 under cold stress (Fig. 4m). Consistent with enhanced oxidative stress management, 3,3′-diaminobenzidine (DAB) and nitroblue tetrazolium (NBT) staining revealed substantially lower accumulation of, $H_2O_2$ and $O_2$ in the mutant leaves (Fig. 4n).

Together, these data demonstrate that disrupting TPP riboswitch confers broad-spectrum and robust resistance to *Magnaporthe oryzae* infection across multiple geographical strains and inoculation methods, while simultaneously enhancing cold tolerance through improved management of oxidative stress.

## Rewiring of transcriptional-metabolic networks drives multi-trait enhancement

To confirm that the observed multitrait improvements were indeed due to the function of the *OsTHIC* gene rather than off-target effects, we generated two independent *OsTHIC* overexpression lines (OE1 and OE2; Supplementary Fig. 11a) and further tested them under *Magnaporthe oryzae* infection and cold stress. Both OE lines exhibited enhanced resistance to *M. oryzae* (Supplementary Fig. 11b-c) and cold tolerance (Supplementary Fig. 11d-f). These results, combined with those from the gene-edited lines, demonstrate that *OsTHIC* confers rice tolerance to multiple stresses, thereby validating the on-target nature of the riboswitch editing.

To test whether enhanced phenotypes in the riboswitch-edited lines were resulted from increased vitamin B1 content, we treated rice plants at the grain-filling stage with 1 mM TPP for 14 days. Metabolite profiling of endosperm revealed that, similar to the *trs*-edited lines, the contents of thiamine, riboflavin, niacin, pantothenic acid, pyridoxine, α-tocopherol, lysoPE 18:3, lysoPC 18:3, leucine, threonine, serine, and valine were significantly upregulated in the two TPP-treated plants compared with the control (Fig. 5a). Similarly, we exogenously applied 1 mM TPP at the five-leaf stage, followed by challenge with *M. oryzae* or cold stress. Consistent with the phenotypes of the riboswitch-edited lines, the TPP-treated plants exhibited significantly enhanced resistance to rice blast (Fig. 5b-d) and improved cold tolerance compared with the control (Fig. 5e, f).

To elucidate the mechanism by which riboswitch editing enhances vitamin B1 accumulation, we performed, we employed transient expression assays in rice protoplasts. The 3′-UTR regions from the wild-type (3′-UTR$^{WT}$) and edited lines (M1-M9, corresponding to 3′-UTR$^{trs1}$ to 3′-UTR$^{trs9}$) were cloned into a dual-luciferase reporter system (Fig. 5g left). Upon treatment with 1 mM TPP, all nine mutant 3′-UTRs produced significantly higher luciferase activity than 3′-UTR$^{WT}$. The 3′-UTR$^{trs3}$ and 3′-UTR$^{trs8}$ exhibited the greatest increases in reporter activity (Fig. 5g right), consistent with their highest thiamine accumulations in vivo (Fig. 1b–d). These results confirm that editing the *THIC* TPP-riboswitch sequence alleviate TPP-mediated feedback inhibition, thereby upregulating vitamin B1 biosynthesis.

To investigate the molecular mechanism underlying the comprehensive enhanced rice in riboswitch gene-edited lines, we performed a transcriptomic analysis of the third leaves of the wild-type and the *trs* lines, with or without 1 mM TPP treatment. TPP treatment in WT tiggered the upregulation of 5842 genes and the downregulation of 1350 genes (Fig. 5h, Supplementary Data 3). Compared with ZH11, the *trs3* and *trs8* lines shared 2346 upregulated and 3536 downregulated genes (Fig. 5i, Supplementary Data 4). *OsTHIC* expression was significantly elevated in both lines (Supplementary Data 4), consistent with the release of feedback inhibition. A comparative analysis of the transcriptional responses to TPP treatment (in WT) and to riboswitch editing (in mutants) identified 724 co-upregulated genes (Fig. 5j). Kyoto Encyclopedia of Genes and Genomes (KEGG) pathway analysis of these 724 genes revealed significant shifts in vitamin metabolism, lipid metabolism, amino acid and nitrogen metabolism, photosynthesis and carbon fixation, and plant-pathogen interaction, all processes linked to nutritional quality, yield, and stress tolerance (Fig. 5k). The expression patterns of key genes in these pathways were validated by qPCR (Fig. 5l). Collectively, these results demonstrate that vitamin B1 modulates transcriptional reprogramming across multiple metabolic and stress-related pathways, underpinning the integrated improvements in agronomic and nutritional traits in rice.

In plants, TPP serves as an essential coenzyme for key enzymes, including pyruvate dehydrogenase complex (PDC), pyruvate dehydrogenase (PDH), and 2-oxoglutarate dehydrogenase (2-OGDH), in the tricarboxylic acid (TCA) cycle (Fig. 5m). We hypothesized that, beyond its transcriptional effects, the altered vitamin B1 levels in *trs* lines could enhance the activity of these TPP-dependent enzymes by increasing TPP availability. Thus, we quantified TPP levels in riboswitch-edited lines and observed a marked increase compared with those in wild-type controls (Fig. 5n). Protein extracts from the mutants indeed showed enhanced activities of PDH (the E1 subunit of PDC) and 2-OGDH activities (Fig. 5o, p), while PDC activity was unchanged (Supplementary Fig. 12). Metabolite profiling of central pathways associated with these enzymes revealed 20 significantly increased metabolites in the *trs* lines, including essential amino acids, TCA intermediates such as pyruvate and succinate, and chorismite, a precursor of multiple metabolites (Fig. 5q). We observed a pronounced increase in cAMP, a second messenger involved in growth and stress signaling[42,45,46], whose synthesis is indirectly influenced by vitamin B1. These results further support the role of TPP-mediated metabolic rewiring in enhancing both developmental and defence processes.

Together, our results demonstrate that targeted riboswitch editing perturbs cellular TPP homeostasis, activates central carbon metabolism, and amplifies connected upstream and downstream pathways. This rewiring of transcriptional-metabolic networks through enhanced TPP availability stimulates TPP-dependent enzymatic hubs and directs carbon flux towards growth- and defence-related metabolism, providing a mechanistic basis for the observed improvements in quality, yield, and stress tolerance.

## Conserved TPP riboswitch function enables multigenic improvement in tomato

Given the promising results in rice, we asked whether elevating vitamin B1 levels through riboswitch editing could also be effective in dicots. We therefore generated two lines with edited TPP riboswitch in the *SlTHIC* gene, named *sltrs1* (single-base insertion) and *sltrs5* (five-base deletion) (Supplementary Fig. 13). Both mutants displayed elevated vitamin B1 contents (Fig. 6b) and increased levels of numerous other nutrient metabolites including riboflavin, niacin, pantothenic acid, pyridoxine, α-tocopherol, monoacylglycerol phospholipids, and several essential amino acids (Fig. 6a-m, Supplementary Data 5).

The edited lines showed improved vegetative growth (Fig. 6n) and a striking enhancement in photosynthetic performance, with photosynthetic rates raised by 56.46–77.05% (Fig. 6o). This was accompanied by increased transpiration (Fig. 6p) and stomatal conductance (Fig. 6r), whereas internal carbon dioxide concentration remained

https://doi.org/10.1038/s41467-026-69730-4

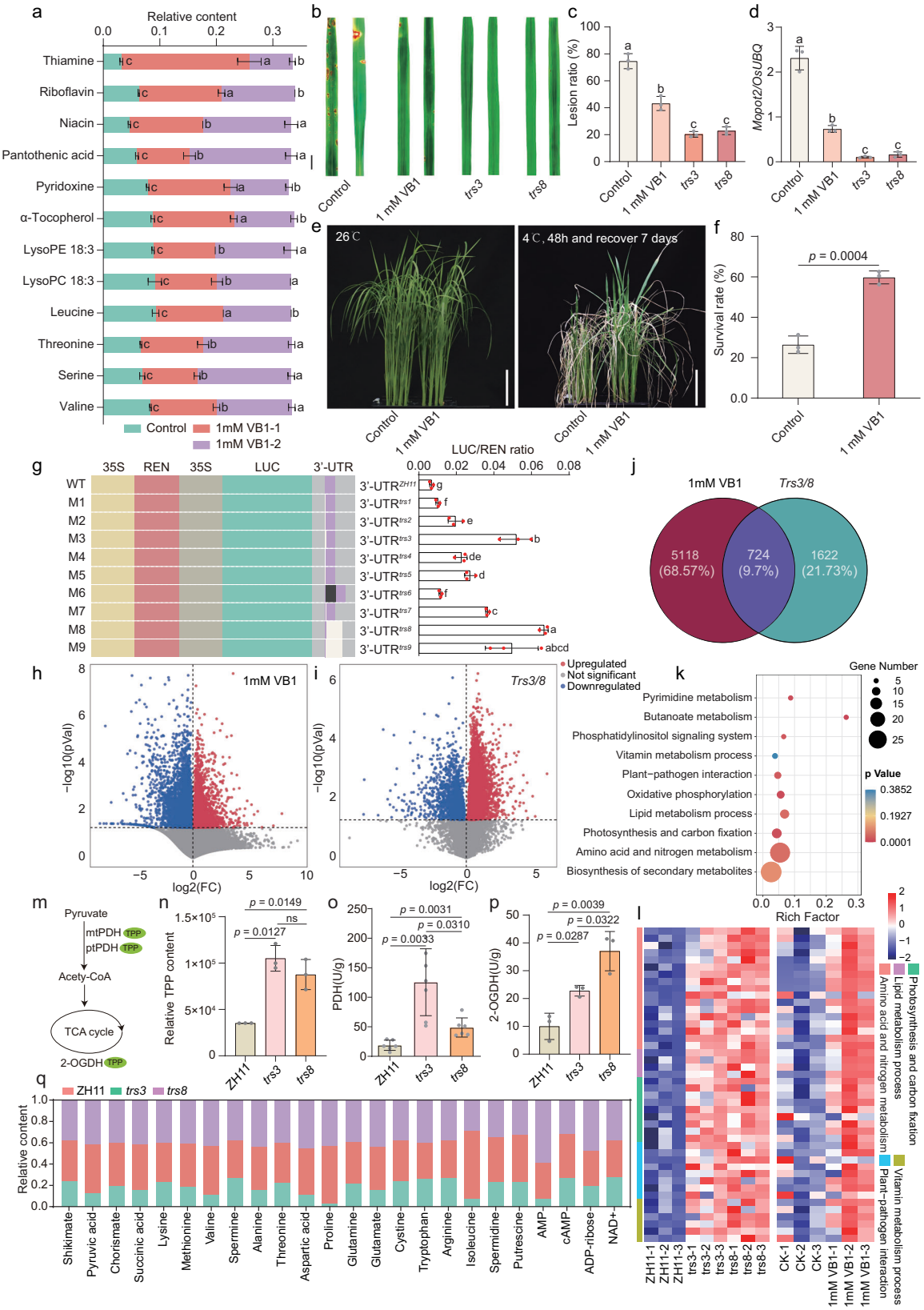


unchanged (Fig. 6q). In addition, the mutants also exhibited clear resistance to *Botrytis cinerea* under both natural (Fig. 6s) and artificial inoculation conditions (Fig. 6t-v). Similar to the research conducted in rice, we also evaluated the performance of tomato *sltrs* plants under LT stress. After exposure to LT stress, compared with WT plants, *sltrs1* and *sltrs5* plants exhibited a more robust phenotype (Fig. 6w), lower ROS accumulation (Fig. 6x, y), and lower electrolyte leakage (Fig. 6z), indicating that the gene-edited of TPP riboswitch conferred enhanced cold tolerance to the tomato plants.

Taken together, these results demonstrate that TPP riboswitch-mediated editing of *SlTHIC* in tomato effectively enhances nutritional composition, photosynthetic capacity, and multi-stress resilience,

**Fig. 5 | Multidimensional regulation of TPP riboswitch editing drives crop enhancement. a** Quantification of nutritional metabolites in the filling-stage endosperm of ZH11 with (1 mM VB1-1 and 1 mM VB1-2) or without (Control) exogenous TPP treatment. **b**–**d** Disease evaluation in rice lines after inoculation with *M. oryzae* ZB25. Lesion formation (c) and fungal biomass (d) in ZH11, TPP-treated ZH11 (VB1), *trs3*, and *trs8* were determined at 10 days post-inoculation. Fungal growth was quantified by qRT-PCR analysis of *Mopot2* expression in inoculated leaves, normalized to rice *OsUbQ*. **e** Cold-stress phenotypes of ZH11 plants with and without TPP treatment. **f** Survival rate of ZH11 plants with or without TPP treatment after cold stress treatment. **g** Dual-luciferase reporter assays evaluating the activity of the 3′-UTR with nine edited TPP riboswitch variants in rice protoplasts. **h**, **i** Volcano plots comparing differentially expressed genes (DEGs) in TPP-treated versus untreated groups and in wild-type versus *trs* mutant lines. Red and blue dots represent upregulated and downregulated genes, respectively ($P \le 0.05$). **j** Venn diagram of upregulated genes shared between TPP-treated and *trs* lines. **k** KEGG pathway enrichment analysis for upregulated genes shared between TPP-treated and *trs* lines. **l** RT-qPCR analysis of DEGs associated with photosynthesis, carbon fixation, and metabolic processes (lipid, amino acid, vitamin) as well as plant-pathogen interactions. Expression was quantified in leaves of ZH11, trs3, and trs8 lines, with or without 1 mM TPP treatment, at the five-leaf stage. Data for each row is standardized by *Z*-score. **m** Schematic diagram of key metabolic pathways involved in TPP-dependent enzymes. **n** Relative TPP content in leaves of ZH11, *trs3* and *trs8* lines during the five-leaf stage. **o**, **p** Assay of Pyruvate Dehydrogenase and 2-Oxoglutarate Dehydrogenase activities in crude protein extracts from gene-edited lines. **q** Alterations in metabolite levels of TPP-dependent core metabolism linked to plant growth, development, and resistance in *trs* mutants. Data are presented as mean ± SD, with error bars show variability among biological replicates, and gray dots indicate individual samples. Data in (**a**, **c**, **d**, **f**, **g**, **n**, **p**) ($n = 3$ per line), in (**o**) ($n = 7$ per line). All statistical tests were carried out using a one-way ANOVA, with distinct letters indicating signficant differences ($P < 0.05$). Source data are provided as a Source Data file.

confirming the broad applicability and translational potential of this strategy beyond monocot species.

## Discussion

Our study demonstrated that targeted editing of the TPP riboswitch in the 3′-UTR of *THIC* represents a highly effective strategy for simultaneously improving nutritional quality, yield, and stress tolerance in crops. We observed that CRISPR-Cas9-induced mutations in the riboswitch region led to a significant increase in vitamin B1 content in rice grains-up to 5.5 mg $kg^{-1}$, which is substantially higher than the typical concentration of 1 mg $kg^{-1}$ found in conventional polished rice. This elevation implies that approximately 300 g of rice from the edited lines would suffice to meet the daily recommended intake of vitamin B1 for adults, offering a practical solution to mitigate deficiencies that affect nearly two billion people worldwide[47,48]. In addition to thiamine, we documented broad-spectrum enhancements in other essential nutrients, including B vitamins (riboflavin, niacin, pantothenic acid, pyridoxine), α-tocopherol (vitamin E), phospholipids, and multiple essential amino acids. All of these compounds are highly important for human health[49]. This multi-nutrient fortification effectively addresses the complex nature of "hidden hunger," which often involves concurrent deficiencies in several micronutrients.

The agronomic benefits of the riboswitch edits were equally remarkable. Field trials conducted across diverse environments (Wuhan and Sanya) have consistently shown yield increases of 19.29–20.77% in edited lines, primarily attributable to improved panicle architecture—longer panicles with more grains—rather than changes in tiller number or grain weight. Importantly, these gains were achieved without compromising nitrogen use efficiency; under low-nitrogen conditions, the edited lines maintained superior growth, chlorophyll content, and biomass accumulation, indicating a more efficient metabolic platform. These phenotypic improvements are underpinned by significant enhancements in photosynthetic parameters, including higher net photosynthetic rates (Pn), maximal photochemical efficiency (Fv/Fm), and electron transport rates (ETRs). We propose that increased TPP availability enhances the activity of key enzymes in the Calvin–Benson and TCA cycles, thereby promoting carbon fixation and energy metabolism.

A key finding of this study is the concurrent increases in of biotic and abiotic stress tolerance in riboswitch-edited lines. We observed strong resistance to rice blast *(Magnaporthe oryzae*) under both field and laboratory conditions, with reduced lesion formation and fungal biomass accumulation. This finding is consistent with the established role of thiamine as a priming agent for systemic acquired resistance[30,34]. Similarly, the edited lines exhibited pronounced cold tolerance, which was likely mediated by reduced membrane damage (as indicated by lower electrolyte leakage) and decreased reactive oxygen species (ROS) accumulation under low-temperature stress. These results align with transcriptomic data showing the upregulation of genes involved in pathogen response, chloroplast function, and metabolic pathways (such as like lipid, and amino acid metabolism) related to membrane maintenance.

At the molecular level, our multi-omics analyses revealed that the riboswitch edits triggered extensive transcriptional and metabolic reprogramming. RNA-seq profiling revealed the upregulation of genes associated with vitamin metabolism, photosynthesis, amino acid and lipid biosynthesis, and stress responses, collectively supporting the observed phenotypic advantages. Importantly, enzymatic assays confirmed the increased activities of TPP-dependent enzymes such as pyruvate dehydrogenase (PDH) and 2-oxoglutarate dehydrogenase (2-OGDH), corroborating the role of TPP as a central metabolic coordinator. The resulting shifts in metabolite pools, including elevated levels of pyruvate, succinate, chorismate, essential amino acids, and the second messenger cAMP—further illustrate the profound metabolic rewiring induced by increased TPP availability.

Our mutational analysis revealed a clear structure-function relationship in the TPP riboswitch regulatory mechanism of the TPP riboswitch. The large fragment complete deletion of the riboswitch sequence in *trs8* and the specific mutation in *trs3* resulted in the strongest constitutive expression, indicating near-complete loss of TPP responsiveness. The other mutant lines exhibited graded responses corresponding to their specific alterations: *trs7* (6 bp deletion), *trs5* (2 bp deletion), *trs4* (4 bp deletion), *trs2* (3 bp deletion), *trs6* (241 bp insertion), and *trs1* (1 bp deletion) showed progressively weaker effects on luciferase activity. This stepwise pattern of reporter activity directly correlates with the extent of structural perturbation to the conserved aptamer domain. The consistent structure-activity relationship across the mutant series provides strong evidence that the phenotypic differences arise from specific, targeted alterations to the riboswitch rather than nonspecific genetic changes, demonstrating that even single-nucleotide alterations can significantly impair TPP binding and regulatory function.

Notably, we also validated the cross-species applicability of this approach by editing the homologous riboswitch in tomato. The resulting mutants exhibited similar pleiotropic benefits, including elevated nutrient levels, improved photosynthetic performance, and enhanced resistance to *Botrytis cinerea*. This consistency across distantly related species underscores the evolutionary conservation of TPP riboswitch function and suggests broad utility in dicot and monocot crops.

A pertinent question arising from our findings is why such beneficial mutations have not been fixed in natural populations despite the conservation of the TPP riboswitch. We speculate that the persistence

https://doi.org/10.1038/s41467-026-69730-4

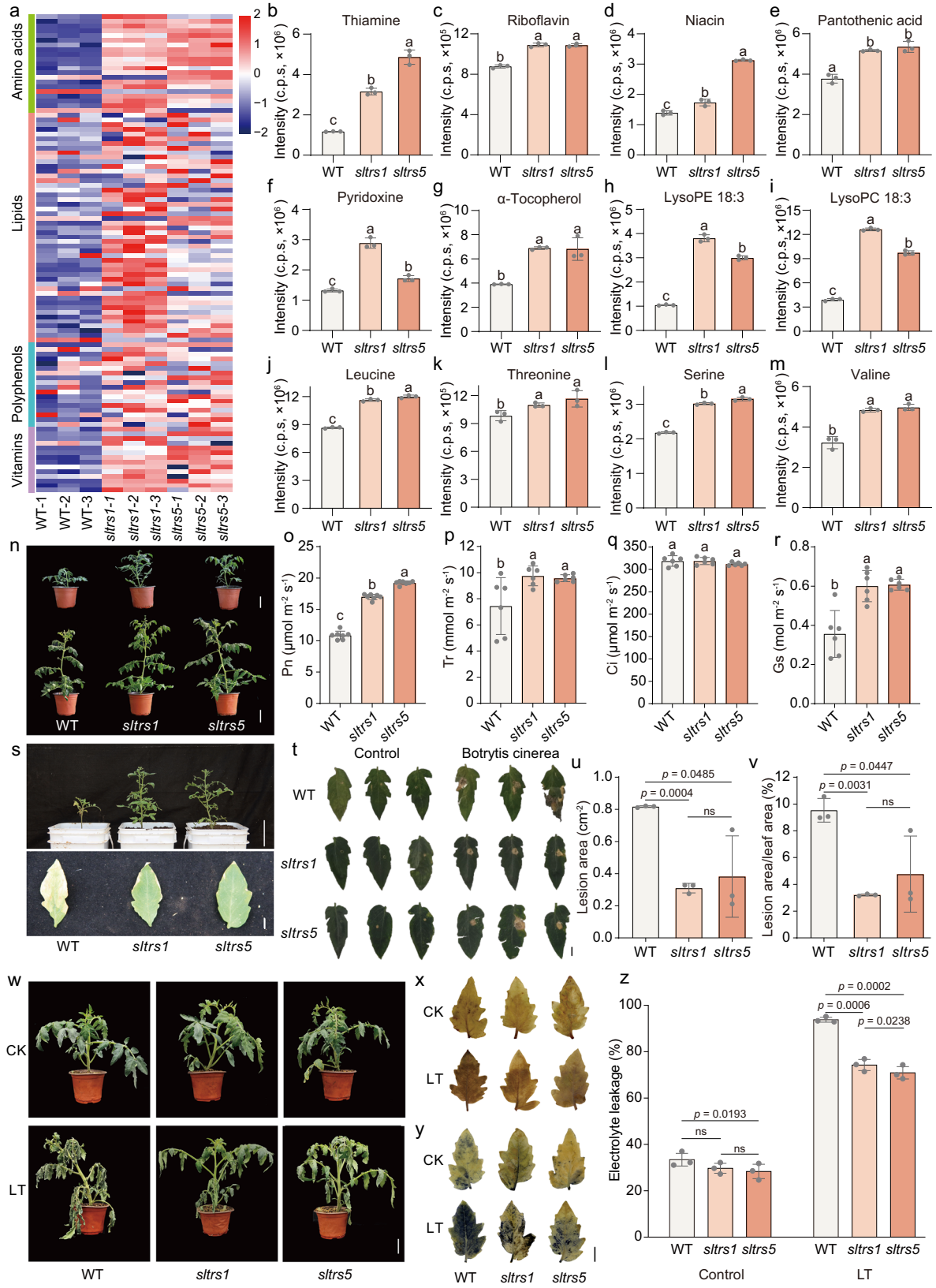


of the functional riboswitch in natural populations may be attributed to fitness trade-offs under different environmental conditions. In natural ecosystems, where nutrients are often limited and stresses are variable, constitutive overexpression of thiamine biosynthesis, such as that caused by riboswitch disruption, could lead to metabolic imbalance or unnecessary energy expenditure, reducing overall fitness. Therefore, the riboswitch mechanism may have been conserved to finely tune thiamine homeostasis in response to fluctuating environments, preventing potential costs of overexpression in resource-limited or stress-free settings. Conversely, in modern agricultural systems, with ample nutrient supply and managed environmental pressures, such trade-offs can be mitigated, allowing the beneficial

**Fig. 6 | The gene-edited TPP riboswitch improves quality, photosynthesis and stress tolerance in tomato. a** Overview of nutrient metabolome distribution of WT and the *sltrs1* and *sltrs5* mutant lines. Data for each row is standardized by *Z*-score. **b**–**m** Quantification of thiamine, riboflavin, niacin, pantothenic acid, pyridoxine, α-tocopherol, lysoPE 18:3, lysoPC 18:3, leucine, threonine, serine, valine in fruits of WT, *sltrs1* and *sltrs5* lines. Phenotypes of WT, *sltrs1* and *sltrs5* lines. Scale bar = 10 cm. **n**, Overview of plant architecture for the WT, *sltrs1* and *sltrs5* lines under natural growth conditions. **o** Gas exchange parameter (Pn) of WT, *sltrs1* and *sltrs5* lines. **p** Transpiration rate (Tr) of WT, *sltrs1* and *sltrs5* lines. **q** Intercellular CO2 concentration (Ci) of WT, *sltrs1* and *sltrs5* lines. **r** Stomatal conductance (Gs) of WT, *sltrs1* and *sltrs5* lines. **s** Phenotypes of WT, *sltrs1* and *sltrs5* lines under natural disease pressure. Scale bar = 10 cm and 1 cm. **t** Leaves phenotypes of WT, *sltrs1* and *sltrs5* lines under artificial exposure to *Botrytis cinerea*. **u** Lesion area of WT, *sltrs1* and *sltrs5* lines under artificial exposure to *Botrytis cinerea*. **v** The ratio of lesion area to leaf area of WT, *sltrs1* and *sltrs5* lines under artificial exposure to *Botrytis cinerea*. **w** Phenotypes of WT, *sltrs1* and *sltrs5* lines under control (CK) and Low temperature (LT) stress (bar, 5 cm). **x**, **y** DAB (**x**) and NBT (**y**) staining of WT, *sltrs1* and *sltrs5* leaves under CK and LT stress. **z** Elextrolyte leakage of WT, *sltrs1* and *sltrs5* leaves under CK and LT stress. Data are the means of three or six replicates, with standard errors shown by vertical bars. Bars represent mean ± SD, with error bars show variability among biological replicates, and gray dots indicate individual samples. Data in (**b**-**m**, **u**, **v**, **z**) ($n = 3$ per line), in (**o**) ($n = 7$ per line), in (**p**–**r**) ($n = 6$ per line). All statistical tests were carried out using a one-way ANOVA, with distinct letters indicating signficant differences ($P < 0.05$). Source data are provided as a Source Data file.

effects of riboswitch editing to be fully expressed without compromising plant vigour.

It is also important to consider the practical implications of our approach in the context of crop biotechnology. Unlike traditional transgenic strategies that often involve the introduction of foreign genes, our method relies on precise editing of endogenous regulatory elements. This may facilitate regulatory approval and public acceptance, as exemplified by the recent development of similar genome-edited crops with improved nutritional profiles[50]. That said, the eventual deployment of such crops will still require careful evaluations of long-term agronomic performance, environmental impact, and socioeconomic feasibility.

In conclusion, our work establishes riboswitch-mediated metabolic rewiring as a powerful strategy for breaking the yield–quality–resilience trade-off in crops. By elevating cellular TPP levels through a single genetic intervention, we achieved coordinated improvements in nutrition, productivity, and stress adaptation—a triple benefit that has proven elusive in conventional breeding and transgenic approaches. We propose that this strategy could be extended to other vitamins and metabolic pathways, offering a general paradigm for the next generation of biofortified, climate-resilient crops.

## Methods

### Plant material and field trials investigation

The *trs* mutant constructs were generated via CRISPR-Cas9 technology[51]. For the *OsTHIC* overexpression construct, the full-length coding sequence was amplified from the japonica cultivar Nipponbare and cloned into the binary vector pJC034 using Gateway recombination reactions (Invitrogen, Waltham, MA, USA). The generated vectors were introduced into the calli of Zhonghua11 (ZH11), via *Agrobacterium tumefaciens*-mediated transformation. Field yield was assessed at the Wuhan and Sanya experimental stations (low incidence of rice blast) and resistance to blast was evaluated in the Taojiang and Enshi blast nurseries (high incidence of rice blast) during the summer season. Enshi (Hubei Province) and Taojiang (Hunan Province) were selected because this mountainous area has a high incidence of rice blast disease each year. Field plots were designed following the strategy established by the International Rice Research Institute. For each field trial, plants were grown with either 5 replicate plots for each line, and each plot contained 100 plants that were 20 cm apart. Diseased plantlets of the blast-susceptible line Lijiangxintuanheigu were used as a source of inoculum for spreading the disease. One row of Lijiangxintuanheigu was sown for every 10 rows of test accessions, and the disease was allowed to spread naturally by wind dispersal. In the normal fields, we did not include a spreader row. The rice blast resistance levels of different lines were evaluated according to the International Rice Research Institute evaluation system, and the percentage of necrotic panicles caused by blast was calculated. For the cold stress, *trs* lines and Zhonghua11 (ZH11) seedlings were grown in black pots in an optical incubator at 28 °C with a 16-h light/8-h dark photoperiod and 70% relative humidity. Fifteen-day-old seedlings were subjected to 4 °C treatment for 48 hours and then transferred to 28 °C or recovery conditions.

### Preparation of metabolic samples

The samples were first freeze-dried and then ground into powder using a mixer mill (MM400, Retsch) for 1.5 min at 30 Hz. Subsequently, 100 mg of the resulting powder was weighed and extracted overnight at 4 °C with pure methanol. The extracts were then centrifuged for 10 min at 10,000 × *g*. The supernatants were collected, followed by filtration (SCAA-104, 0.22 μm pore size; ANPEL Shanghai, China, www.anpel.com.cn/) before LC–MS analysis. To establish a specific metabolic database of brown rice, samples were mixed into multiple samples for widely targeted metabolomics analysis[52,53].

### Metabolites quantification

For metabolites content analysis, samples were analysed using a high-performance liquid chromatography (HPLC) staple targeted method[54,55]. The analytical conditions were as follows, HPLC: column, shim-pack GISS C18 (pore size 1.9 μm, length 2.1 × 100 mm); solvent system, water (0.04% acetic acid): acetonitrile (0.04% acetic acid); gradient program, 0 min, 5% B; 12.0 min, 95% B; 13.2 min, 95% B; 13.3 min, 5% B; 15.0 min, 5% B; flow rate, 0.4 mL $min^{-1}$; temperature, 40 °C; and injection volume, 2 μL. Targeted metabolic profiling analysis was performed using a scheduled multiple reaction monitoring (MRM) via an LC-ESI-QQQ-MS/MS system (LCMS-8060, SHIMADZU, Japan). The ESI source operation parameters were as follows: nebulizing gas flow, 3 L $min^{-1}$; heating gas flow, 10 L $min^{-1}$; interface temperature, 500 °C; DL temperature, 250 °C; heat block temperature, 400 °C; and drying gas flow, 10 L $min^{-1}$. The data recorded were processed with LabSolutions 5.91 software.

### Determination of protein content and starch content in polished rice

To determine the protein and starch contents in polished rice, we employed standard biochemical methods. For protein content, we used the Kjeldahl method, which involves digestion of the rice sample with concentrated sulfuric acid to convert the nitrogen in the proteins to ammonium sulfate. The resulting solution was then distilled to release ammonia, which was subsequently titrated with a standard acid solution to quantify the nitrogen content. The protein content was then calculated based on the nitrogen content, assuming an average nitrogen-to-protein conversion factor of 6.25. To determine the starch content, we utilized the anthrone reagent method. This method involves hydrolysing the starch in the rice sample to glucose using an acid hydrolysis procedure. The resulting glucose was then reacted with anthrone reagent, which formed a blue-green complex. The intensity of this complex was measured spectrophotometrically at 620 nm, and

the starch content was determined by comparing the absorbance to a standard glucose curve. Both methods were performed in triplicate to ensure the accuracy and reproducibility of the results. The protein and starch contents are expressed as percentages of the total weight of the polished rice sample.

### Low-nitrogen treatment

Low-nitrogen treatment was applied after sowing, germination, and normal growth for 10 days. For the low-nitrogen group, 20% of the normal nitrogen level was supplemented, while the other conditions remained consistent with those of the control group. After one month of treatment, the plants were harvested to analyse their biomass theirand chlorophyll content. The plants subjected to low-nitrogen conditions throughout their entire growth period were cultivated under low-nitrogen conditions until heading and seed setting, after which parameters such as plant height, root length, and tiller number were statistically analysed. The nutrient solution for all the plants was replaced every three days.

### Rice plant infection assays

*M. oryzae* strains were isolated from rice fields in Enshi (ES67) and Liaoning (LN3, LN13) in China, and ZB25 was stored in the laboratory. Four- to five-week-old rice plants at the tillering stage were used for all inoculations. For spray inoculation, the plants were first acclimated in a humidity chamber (>90% relative humidity) for 24 h to increase their susceptibility. *M. oryzae* was cultured on oatmeal agar plates at 25 °C under continuous light for 10-14 days to induce sporulation. Spores were harvested by gently scraping the culture surface with sterile water containing 0.01% (v/v) Tween-20. The resulting suspension was filtered through two layers of sterile cheesecloth to remove mycelial debris, and the spore concentration was adjusted to $1\times10^5$ spores/mL using a haemocytometer. The spore suspension was evenly sprayed onto both adaxial and abaxial leaf surfaces using an atomizer until run-off (approximately 10 mL per plant). A negative control group, sprayed with 0.01% Tween-20 solution, was included. For punch inoculation, spores were collected from 10-day-old cultures as described above, and the concentration was adjusted to $1\times10^5$ spores/mL with 0.025% Tween-20. Fully expanded leaves of 30-day-old plants were wounded with a sterile punch and inoculated with a 10 µL droplet of the spore suspension. The inoculated site was subsequently sealed with clear tape to maintain humidity. All inoculated plants were transferred to a greenhouse for disease development. Symptoms were assessed at 10 days post-inoculation (dpi), and fungal biomass was quantified by quantitative PCR (qPCR)[56,57].

### Measurement of leaf gas exchange parameters

Photosynthesis parameters, such as the net photosynthetic rate (Pn), stomatal conductance (Gs), intercellular $CO_2$ concentration (Ci), and transpiration rate (Tr) of leaves were measured at 10:00–11:00 am using the portable photosynthesis system LI-6800 (LI-COR Biosciences, Lincoln, USA). The level of irradiance used to activate photosynthesis was 600 µmol $m^{-2}$ $s^{-1}$. All measurements were performed on the youngest fully expanded flag leaf of each plant. The atmospheric $CO_2$ concentration and temperature were approximately 400 µmol·$mol^{-1}$ and 25 °C, respectively.

### Measurement of chlorophyll fluorescence

The in vivo chlorophyll fluorescence of leaves was measured using a PAM-2500 (Heinz Walz, Effeltrich, Germany) at room temperature (approximately 25 °C). Before measurement, the plants were dark adapted for 30 min. The light-adapted fluorescence parameters were recorded for the PPFDs (387 µmol photons $m^{-2}$ $s^{-1}$, 635 nm). The intensity and duration of the light saturation pulse used to measure Fm were 10,000 µmol photons $m^{-2}s^{-1}$ and 300 ms, respectively. The chlorophyll fluorescence parameters were calculated as follows:

$$Fv/Fm = (Fm - Fo)/Fm \quad (1)$$

$$Y(II) = (Fm' - Fs)/Fm' \quad (2)$$

$$Y(NO) = Fs/Fm \quad (3)$$

$$NPQ = (Fm - Fm')/Fm' \quad (4)$$

$$qP = (Fm' - Fs)/(Fm' - Fo') \quad (5)$$

$$ETR = Y(II) \times PAR \times 0.84 \times 0.5 \quad (6)$$

Fo and Fm are the minimum and maximum fluorescence after dark adaptation, respectively. Fo' and Fm' represent the minimum and maximum fluorescence after light adaptation, respectively. Fs is the light-adapted steady-state fluorescence[58].

### Chlorophyll content analysis

Fresh leaf blades were collected, frozen in liquid nitrogen and ground into fine powder. Pigments were then extracted with 80% acetone and shaken overnight in the dark. After centrifugation at 12 000 × *g* for 10 min at 4 °C, the absorbance of the supernatant was measured at 663 and 645 nm and reported as $OD_{663}$ and $OD_{645}$, respectively.

### Electrolyte leakage assay

Three uniformly sized leaf fragments were collected from each sample, cut into smaller pieces, rinsed, and shaken in deionized water overnight. After incubation, the electrical conductivity of the solution (R1) was measured using a DDS-11C conductivity meter (Shanghai Leici Instrument Inc., Shanghai, China). The samples were then heated in boiling water in a sealed vessel for 20 min, and the conductivity (R2) was measured again. Electrolyte leakage was calculated as follows:

$$\text{Electrolyte leakage} = (R1)/(R1 + R2) \quad (7)$$

### NBT and DAB staining

$O_2^-$ and $H_2O_2$ were detected using nitroblue tetrazolium chloride (NBT; Sangon Biotech, Shanghai, China) and 3,3′-diaminobenzidine (DAB; Sangon Biotech) staining, respectively. To detect $O_2^-$, 3-5 cm leaf blades were harvested and incubated in 1% NBT (w/v, pH=7.8) and vacuum infiltrated for 30 min. After being incubated in the dark at room temperature, the samples were transferred to 95% ethanol at 80 °C to remove the chlorophyll. To detect $H_2O_2$, plant leaves were stained with 0.05% DAB (w/v, pH 3.8), vacuum infiltrated for 30 min and then incubated for 12 h. Subsequently, all the stained leaves were transferred to 95% ethanol and incubated at 80 °C until the decolorizing solution was colourless.

### Tomato material generation and low-temperature treatment

Tomato TPP riboswitch gene editing (*Sltrs*) plants were obtained by CRISPR/Cas9 technology[59]. The WT tomato plants used in this study were of the 'Ailsa Craig' ecotype, whereas the transgenic tomato plants were obtained by *A. tumefaciens*-mediated transformation. The *Sltrs* mutants were identified by PCR and confirmed by DNA sequencing. Tomato seeds were germinated and grown in pots under cool-white fluorescent light (600 mmol $m^{-2}$ $s^{-1}$, 12 h photoperiod) at 28 °C: 18 °C (day: night) and 60% relative humidity in a growth chamber (KuLan,

China). During the low-temperature treatment, six-leaf-one-heart plants were placed under 4 °C conditions, with normal growth conditions serving as the control. After 48 h, record the phenotypes were recorded, and the resistance index was measured.

### Tomato leaf pathogen infection

*Botrytis cinerea* infection followed the method of Zaid et al.[60] with modifications. Specifically, *Botrytis cinerea* (Bc, isolate BcI16) cultures were maintained on potato dextrose agar (PDA) (Difco Lab) plates and incubated at 22 °C for 5 to 7 days. *Botrytis cinerea* spores were harvested from PDA plates supplemented with 1 mg $mL^{-1}$ glucose and 1 mg $mL^{-1}$ $K_2HPO_4$ and filtered through gauze. The spore concentration was adjusted to $10^6$ spores $mL^{-1}$ using a haemocytometer. Inoculate 10 μL of spore suspension into the fourth to fifth leaves of tomato plants aged 5-7 weeks. The inoculated plants were kept in a humid growth chamber at 22 °C. The control consisted of plants or leaves treated with water/buffer. The area of necrotic lesions was measured 5-7 days after inoculation.

### Reporting summary

Further information on research design is available in the Nature Portfolio Reporting Summary linked to this article.

## Data availability

The metabolomics and transcriptomics data generated in this study have been deposited in the OMIX, China National Center for Bioinformation/Beijing Institute of Genomics, Chinese Academy of Sciences, under accession number OMIX009553 and OMIX009554, respectively. Source data are provided with this paper.

## References


1. von Braun, J. et al. Food systems: seven priorities to end hunger and protect the planet. *Nature* **597**, 28–30 (2021).
2. Gashu, D. et al. The nutritional quality of cereals varies geospatially in Ethiopia and Malawi. *Nature* **594**, 71–75 (2021).
3. Sreenivasulu, N. et al. Metabolic signatures from genebank collections: an underexploited resource for human health? *Annu Rev. Food Sci. T* **14**, 183–202 (2023).
4. Martin, C. A role for plant science in underpinning the objective of global nutritional security? *Ann. Bot.-Lond.* **122**, 541–553 (2018).
5. Fernie, A. R. & Yan, J. De Novo Domestication: An alternative route toward new crops for the future. *Mol. Plant* **12**, 615–631 (2019).
6. Jiang, L. et al. Regulation of plant vitamin metabolism: Backbone of biofortification for the alleviation of hidden hunger. *Mol. Plant* **14**, 40–60 (2021).
7. Fitzpatrick, T. B. & Chapman, L. M. The importance of thiamine (vitamin B1) in plant health: From crop yield to biofortification. *J. Biol. Chem.* **295**, 12002–12013 (2020).
8. Jing, W. et al. A single transcription factor promotes both yield and immunity in rice. *Science* **361**, 1026–1028 (2018).
9. Ye, X. et al. Engineering the provitamin A (beta-carotene) biosynthetic pathway into (carotenoid-free) rice endosperm. *Science* **287**, 303–305 (2000).
10. Tian, Y. S. et al. Riboflavin fortification of rice endosperm by metabolic engineering. *Plant Biotechnol. J.* **19**, 1483–1485 (2021).
11. Mangel, N. et al. Enhancement of vitamin B(6) levels in rice expressing Arabidopsis vitamin B(6) biosynthesis de novo genes. *Plant J.* **99**, 1047–1065 (2019).
12. Storozhenko, S. et al. Folate fortification of rice by metabolic engineering. *Nat. Biotechnol.* **25**, 1277–1279 (2007).
13. Li, J. et al. Biofortified tomatoes provide a new route to vitamin D sufficiency. *Nat. Plants* **8**, 611–616 (2022).
14. Hurst, J. P. et al. Editing the 19 kDa alpha-zein gene family generates non-opaque2-based quality protein maize. *Plant Biotechnol. J.* **22**, 946–959 (2024).
15. Zhu, Q. et al. Development of "Purple Endosperm Rice" by Engineering Anthocyanin Biosynthesis in the Endosperm with a High-Efficiency Transgene Stacking System. *Mol. Plant* **10**, 918–929 (2017).
16. Zhu, Q. et al. From Golden Rice to aSTARice: Bioengineering Astaxanthin Biosynthesis in Rice Endosperm. *Mol. Plant* **11**, 1440–1448 (2018).
17. Palmer, A. C. Golden Rice: A Quarter-Century of Innovation, Challenges, and the Promise of Better Nutrition. *J. Nutr.* **2**, S0022–S3166 (2025).
18. Shohael, A. et al. Unlocking Opportunities and Overcoming Challenges in Genetically Engineered Biofortification. *Nutrients* **17**, 518 (2025).
19. Brown, J. K. M. A cost of disease resistance: paradigm or peculiarity? *Trends Genet.* **19**, 667–671 (2003).
20. Chen, L.-Q. et al. Sugar transporters for intercellular exchange and nutrition of pathogens. *Nature* **468**, 527–532 (2010).
21. Berens, M. L. et al. Balancing trade-offs between biotic and abiotic stress responses through leaf age-dependent variation in stress hormone cross-talk. *P Natl. Acad. Sci. Usa* **116**, 2364–2373 (2019).
22. Li, S. et al. Modulating plant growth-metabolism coordination for sustainable agriculture. *Nature* **560**, 595–600 (2018).
23. Wu, W. et al. A single-nucleotide polymorphism causes smaller grain size and loss of seed shattering during African rice domestication. *Nat. Plants* **3**, 17064 (2017).
24. Song, L. et al. Reducing brassinosteroid signalling enhances grain yield in semi-dwarf wheat. *Nature* **617**, 118–124 (2023).
25. Rezvi, H. U. A. et al. Rice and food security: Climate change implications and the future prospects for nutritional security. *Food Energy Secur.* **12**, e430 (2023).
26. Song, X. et al. Targeting a gene regulatory element enhances rice grain yield by decoupling panicle number and size. *Nat. Biotechnol.* **40**, 1403–1411 (2022).
27. Raschke, M. et al. Vitamin B1 biosynthesis in plants requires the essential iron sulfur cluster protein, THIC. *P Natl. Acad. Sci. Usa* **104**, 19637–19642 (2007).
28. Kong, D. et al. *AtTHIC*, a gene involved in thiamine biosynthesis in Arabidopsis thaliana. *Cell Res.* **18**, 566–576 (2008).
29. Li, Y. et al. Two major rice loci determine rice-staple food populations differences in vitamin B1 deficiency levels. *Sci. Bull.* **70**, 1046–1050 (2025).
30. Ahn, I.-P. et al. Vitamin B1 functions as an activator of plant disease resistance. *Plant Physiol.* **138**, 1505–1515 (2005).
31. Mishina, T. E. & Zeier, J. Pathogen-associated molecular pattern recognition rather than development of tissue necrosis contributes to bacterial induction of systemic acquired resistance in Arabidopsis. *Plant J.* **50**, 500–513 (2007).
32. Tripathi, D. et al. Chemical elicitors of systemic acquired resistance—Salicylic acid and its functional analogs. *Curr. Plant Biol.* **17**, 48–59 (2019).
33. Wang, G. et al. Dual Function of Rice *OsDR8* Gene in Disease Resistance and Thiamine Accumulation. *Plant Mol. Biol.* **60**, 437–449 (2006).
34. Huang, W. K. et al. Thiamine-induced priming against root-knot nematode infection in rice involves lignification and hydrogen peroxide generation. *Mol. Plant Pathol.* **17**, 614–624 (2015).
35. Nie, Y. et al. Vitamin B1 THIAMIN REQUIRING1 synthase mediates the maintenance of chloroplast function by regulating sugar and fatty acid metabolism in rice. *J. Integr. Plant Biol.* **64**, 1575–1595 (2022).
36. Miranda, J. A. et al. A bifunctional TPS-TPP enzyme from yeast confers tolerance to multiple and extreme abiotic-stress conditions in transgenic Arabidopsis. *Planta* **226**, 1411–1421 (2007).
37. Wachter, A. et al. Riboswitch Control of Gene Expression in Plants by Splicing and Alternative 3′ End Processing of mRNAs. *Plant Cell* **19**, 3437–3450 (2007).

38. Li, Y. et al. Benefiting others and self: Production of vitamins in plants. *J. Integr. Plant Biol.* **63**, 210–227 (2021).
39. Moulin, M. et al. Analysis of Chlamydomonas thiamin metabolism in vivo reveals riboswitch plasticity. *P Natl. Acad. Sci. USA* **110**, 14622–14627 (2013).
40. Fitzpatrick, T. B. & Chapman, L. M. The importance of thiamine (vitamin B(1)) in plant health: From crop yield to biofortification. *J. Biol. Chem.* **295**, 12002–12013 (2020).
41. Zeng, R. et al. A natural variant of *COOL1* gene enhances cold tolerance for high-latitude adaptation in maize. *Cell* **188**, 1315–1329 (2025).
42. Luo, W. et al. COLD6-OSM1 module senses chilling for cold tolerance via 2′,3′-cAMP signaling in rice. *Mol. Cell* **84**, 4224–4238 e4229 (2024).
43. Whitlow, T. H. et al. An Improved Method for Using Electrolyte Leakage to Assess Membrane Competence in Plant Tissues. *Plant Physiol.* **98**, 198–205 (1992).
44. Jiang, H. et al. Natural polymorphism of *ZmICE1* contributes to amino acid metabolism that impacts cold tolerance in maize. *Nat. Plants* **8**, 1176–1190 (2022).
45. Chen, H. et al. TIR1-produced cAMP as a second messenger in transcriptional auxin signalling. *Nature* **640**, 1011–1016 (2025).
46. Yu, D. et al. TIR domains of plant immune receptors are 2′,3′-cAMP/cGMP synthetases mediating cell death. *Cell* **185**, 2370–2386 (2022).
47. Li, J., Martin, C. & Fernie, A. Biofortification's contribution to mitigating micronutrient deficiencies. *Nat. Food* **5**, 19–27 (2024).
48. Cantwell-Jones, A. et al. Global plant diversity as a reservoir of micronutrients for humanity. *Nat. Plants* **8**, 225–232 (2022).
49. Giovannoni & James, J. J. N. B. Breeding new life into plant metabolism. *Nat. Biotechnol.* **24**, 418 (2006).
50. Zhang, J. et al. Releasing a sugar brake generates sweeter tomato without yield penalty. *Nature* **635**, 647–656 (2024).
51. Liu, X. et al. A simple and efficient cloning system for CRISPR/Cas9-mediated genome editing in rice. *PeerJ* **8**, e8491 (2020).
52. Li, K. et al. A long terminal repeat retrotransposon in the *OsACS6* promoter enhances the epigenetic regulation of lysophospholipid contents in rice grains. *Plant Commun.* **6**, 101375 (2025).
53. Li, Y. et al. The NET locus determines the food taste, cooking and nutrition quality of rice. *Sci. Bull.* **67**, 2045–2049 (2022).
54. Chen, W. et al. Genome-wide association analyses provide genetic and biochemical insights into natural variation in rice metabolism. *Nat. Genet.* **46**, 714–721 (2014).
55. Chen, W. et al. A novel integrated method for large-scale detection, identification, and quantification of widely targeted metabolites: application in the study of rice metabolomics. *Mol. Plant* **6**, 1769–1780 (2013).
56. Shen, S. et al. An *Oryza*-specific hydroxycinnamoyl tyramine gene cluster contributes to enhanced disease resistance. *Sci. Bull.* **66**, 2369–2380 (2021).
57. Sha, G. et al. Genome editing of a rice CDP-DAG synthase confers multipathogen resistance. *Nature* **618**, 1017–1023 (2023).
58. Lu, J. et al. Ubiquitin-mediated degradation of SlPsbS regulates low night temperature tolerance in tomatoes. *Cell Rep.* **43**, 114757 (2024).
59. Shimatani, Z. et al. Targeted base editing in rice and tomato using a CRISPR-Cas9 cytidine deaminase fusion. *Nat. Biotechnol.* **35**, 441–443 (2017).
60. Zaid, R. et al. Gliotoxin, an Immunosuppressive Fungal Metabolite, Primes Plant Immunity: Evidence from Trichoderma virens-Tomato Interaction. *mBio* **13**, e0038922 (2022).


## Acknowledgements

This work was supported by the key project of regional joint fund of the National Natural Science Foundation of China (U22A20476), Basic Research Project in 2023-2310LJ01 of Yazhouwan National Laboratory, the National Natural Science Foundation of China (32401887, 32560151, 32300452, 32500233, 32501942), Science and Technology Innovation 2030 Major Project (2024ZD0408004), the Project of National Key Laboratory for Tropical Crop Breeding (NO. PT2400008492), "111" Project (No. D20024). We thank Guotian Li from Huazhong Agricultural University and Gan Sha from South China Agricultural University for offering the *M. oryzae* strains ES67, LN3 and LN13. We also extend our sincere thanks to Chuanying Fang from Hainan University for his valuable guidance on the research concept.

## Author contributions

J.L. and AR.F. conceived the project and supervised this study. Y.L., K.L., J.Z.L., M.B. and S.S. performed the experiments; H.H., QU.Z., R.Z., C.Y., C.Z., G.W., T.C., and X.L. prepared the materials; Y.L., K.L., J.Z.L, S.S., Z.Y., and J.L. analysed the data; Y.L., K.L., J.Z.L, S.S., AR.F., Q.Z., and J.L. wrote and revised the manuscript. All authors discussed the results and commented on the manuscript. All authors read and approved of its content.

## Competing interests

The authors declare no competing interests.

## Additional information

**Supplementary information** The online version contains supplementary material available at https://doi.org/10.1038/s41467-026-69730-4.

**Correspondence** and requests for materials should be addressed to Shuangqian Shen, Alisdair R. Fernie or Jie Luo.

**Peer review information** *Nature Communications* thanks Maria Faustino, who co-reviewed with Simon StrobbeHong-Qing Ling and the other, anonymous, reviewer(s) for their contribution to the peer review of this work. A peer review file is available.